



Original article

Synthesis and electrochemical properties of environmental free L-glutathione grafted graphene oxide/ZnO nanocomposite for highly selective piroxicam sensing

N. Dhanalakshmi^a, T. Priya^a, S. Thennarasu^b, S. Sivanesan^c, N. Thinakaran^{a,*}

^a Environmental Research Lab, PG and Research Department of Chemistry, Alagappa Government Arts College, Karaikudi, 630 003, Tamil Nadu, India

^b School of Chemistry, Bharathidasan University, Thiruchirappalli, 620 024, Tamil Nadu, India

^c Department of Applied Science and Technology, AC Tech, Anna University, Chennai, 25, India

ARTICLE INFO

Article history:

Received 10 October 2019

Received in revised form

28 November 2019

Accepted 3 February 2020

Available online 6 February 2020

Keywords:

Reduced graphene oxide

Glutathione

ZnO

Piroxicam

Electrochemical sensing

ABSTRACT

A simple and reliable strategy was proposed to engineer the glutathione grafted graphene oxide/ZnO nanocomposite (glutathione-GO/ZnO) as electrode material for the high-performance piroxicam sensor. The prepared glutathione-GO/ZnO nanocomposite was well characterized by X-ray diffraction (XRD), Fourier transform infrared spectrum (FTIR), X-ray photoelectron spectroscopy (XPS), field emission scanning electron microscopy (FE-SEM), cyclic voltammetry (CV), electrochemical impedance spectroscopy (EIS) and differential pulse voltammetry (DPV). The novel nanocomposite modified electrode showed the highest electrocatalytic activity towards piroxicam (oxidation potential is 0.52 V). Under controlled experimental parameters, the proposed sensor exhibited good linear responses to piroxicam concentrations ranging from 0.1 to 500 μM . The detection limit and sensitivity were calculated as 1.8 nM and 0.2 $\mu\text{A}/\mu\text{M}\cdot\text{cm}^2$, respectively. Moreover, it offered excellent selectivity, reproducibility, and long-term stability and can effectively ignore the interfering candidates commonly existing in the pharmaceutical tablets and human fluids even at a higher concentration. Finally, the reported sensor was successfully employed to the direct determination of piroxicam in practical samples.

© 2020 Xi'an Jiaotong University. Production and hosting by Elsevier B.V. This is an open access article under the CC BY-NC-ND license (<http://creativecommons.org/licenses/by-nc-nd/4.0/>).

1. Introduction

Piroxicam (4-hydroxy-2-methyl-N-2-pyridinyl-2H-1, 2-benzothiazine-3-carboxamide 1, 2-dioxide) is a well-known non-steroidal anti-inflammatory, analgesic and antipyretic medication with a long biological half-life [1]. Piroxicam is extensively prescribed for several arthritis and inflammatory illnesses such as osteoarthritis, rheumatoid arthritis, acute muscular pain, ankylosing spondylitis, skeletal disorders and other postoperative dental problems [2,3]. However, its incessant or inappropriate consumption can create crucial problems, like kidney and liver failure and serious gastrointestinal disorders (ulcer, bleeding ulcers) [4]. Meanwhile, piroxicam is found in many water bodies as residuals through drug manufacturing companies and/or human wastes. According to reports, every year more than 180 million

Indians are affected by arthritis and get medical assistance. This prevalence is more predominant than other well-known illnesses like cancer, AIDS and diabetes [5]. From healthcare perspective, developing a simple and accurate quantification of piroxicam is urgently needed to preclude the undesirable effects on human health and also environment.

There are diverse analytical methods customarily employed for the determination of piroxicam, such as spectrofluorimetry [6,7], spectrophotometry [8,9], high-performance liquid chromatography [10], thin layer chromatography [11], liquid chromatography [12] and capillary zone electrophoresis [13]. However, these techniques are very complex with comparatively low precision, and require complicated equipment and restricted onsite access. Contrary to the aforementioned methods, electrochemical technique has aroused much attention owing to its high sensitivity, low cost, operational simplicity and proven capability of on-line environmental monitoring. The main challenge is choosing suitable electrode modifiers for the high-performance electrochemical tracing of drugs [14]. In addition, the availability of substantial amounts of some important biologically and electrochemically active

Peer review under responsibility of Xi'an Jiaotong University.

* Corresponding author.

E-mail address: thinakaran2k@yahoo.com (N. Thinakaran).

compounds like ascorbic acid (AA) and uric acid (UA) in the human body can highly disturb the electrochemical tracing of piroxicam, which makes it difficult to selectively detect the piroxicam molecule in biological fluids. Therefore, selective determination of piroxicam is also the most important one.

The application of transition metal oxide nanomaterials has received much attention in various fields of science and technology. They have peculiar chemical and electrical characteristics due to their size-dependent properties [15,16]. In that respect, ZnO is one of the stable and versatile semiconductors that have acquired keen attention in the fabrication of modified electrodes, especially in biosensor studies. Its non-toxic, biomimetic and fast electron transfer properties make it a suitable matrix for the electrochemical biomolecular sensing [17]. Nevertheless, ZnO coated electrode manifests slower sensing response, lower sensitivity, higher noise to signal ratio and limited concentration range of analyte detection. Hence, the preparation of composite ZnO is very pivotal for achieving greater sensitivity and stable responses.

Recently, several explorers have discovered the versatile benefits of graphene oxide (GO) in drug and biomolecular sensing. GO is a rising protagonist in biomolecular sensing because of its superior physicochemical properties [18–20]. It has a wide range of functional groups like hydroxyl, epoxy and carboxyl groups, which have been warranting as a promising material for the retention and preconcentration of biomolecules, metals, inorganic nanoparticles and drugs on its surface. Even though the functional groups play an adequate role in sensing, its preferable characteristics are mainly associated with a monolayer of two-dimensional honeycomb like carbon lattice structure. However, monolayeric graphene nanosheets have a robust tendency to create an agglomerated multilayered graphitic structure through strong π - π stacking, and van der Waals interactions drastically suppress its potential applications [21,22]. To overcome this barrier, chemical functionalization of GO with an organic molecule such as L-glutathione was introduced into the nanocomposite preparation. It can concurrently reduce the GO and stabilize the monolayers of graphene nanosheets [23]. L-glutathione is a natural antioxidant found in cells of mammalian, plants, fungi and some bacteria. It has an ability to prohibit the oxidation of important cellular compounds from free radicals, heavy metals and reactive oxygen compounds [24]. The glutathione functionalization on GO has initiated the electrostatic repulsion between the terminal carboxylic acids of glutathione and GO, which can make a stable monolayer of graphene nanosheets in any medium through the prevention of aggregation and precipitation.

Herein, we have constructed a novel glutathione-GO/ZnO nanocomposite coated electrode for the selective electrochemical determination of piroxicam. L-glutathione is expected to play the dual role of reducing GO, and as a capping agent to stabilize reduced GO sheets. Till date, reports on chemical reduction of GO using environmentally friendly reagents are relatively few. Very recently Fernández-Merino et al. [25] and Zhu et al. [26] have synthesized graphene nanosheets using vitamin C and reducing sugars as reducing agents, respectively. Taking advantage of these literature into account, herein, we developed a simple approach to the production of reduced graphene nanosheets using L-glutathione. Most importantly, L-glutathione and prepared graphene and ZnO are inexpensive and environmentally friendly, which opens new opportunities in selective piroxicam sensor application. The proposed nanocomposite was well characterized by X-ray diffraction (XRD), Fourier transform infrared spectrum (FTIR), X-ray photoelectron spectroscopy (XPS) and field emission scanning electron microscopy (FE-SEM). In order to ascertain the improved electrocatalytic response of piroxicam, various optimization studies such as scan rate, accumulation time and potential, pH value of buffer solution and a wide range of concentrations have been

investigated. The selectivity nature of glutathione-GO/ZnO modified electrode towards piroxicam in the presence of potentially coexisting compounds and the utilization of real-time application were also studied.

2. Material and methods

2.1. Chemicals and instrumentation

Zinc acetate dihydrate ($\text{Zn}(\text{CH}_3\text{CO}_2)_2 \cdot 2\text{H}_2\text{O}$), graphite powder (+100 mesh), piroxicam and L-glutathione were purchased from Sigma-Aldrich, India. All other chemical reagents were bought from Tokyo Chemical Industry Co., Ltd., Japan, and used as received. Ultrapure water was obtained from Millipore system. Analytical grade magnesium stearate, lactose monohydrate, talc, starch, glucose, urea, dopamine, ascorbic acid (AA), uric acid (UA), folic acid, glycine and L-lysine were procured from Sigma-Aldrich, India. The electrochemical measurements were performed on a Bio-Logic workstation (SP-150, France). The three-electrode system consisted of a bare or modified glassy carbon electrode as working electrode, a platinum wire as auxiliary electrode and silver-silver chloride electrode ($\text{Ag}/\text{AgCl}/3\text{ M NaCl}$) as a reference electrode. GT SONIC professional ultrasonic cleaner and Eutech pH Meter were used for sonication and pH measurement, respectively. The FE-SEM was performed to analyze the surface morphology of prepared samples using TESCAN VEGA-3. The Thermo Scientific K- α KA1066 X-ray photoelectron spectrometer system was used for the chemical analysis of prepared samples. X-ray diffraction characterization was performed using Bruker Germany D8 with $\text{CuK}\alpha$ radiation (1.54 Å). Fourier transform-infrared spectroscopy investigations were recorded by FT/IR-6600 spectrophotometer.

2.2. Synthesis of ZnO nanoparticles

The low-temperature hydrothermal method was followed to synthesize ZnO nanoparticles [27]. Shortly, Zinc acetate dihydrate (0.1 M) was dispersed in ultrapure water (50 mL) and constantly stirred for 3 h. Then, NaOH solution (0.5 M) was slowly poured in the above solution until the pH attained was 8. At this time, the clear solution was gently turned into white suspension and stirred for another 2 h. After that, the suspension was taken in teflon-lined stainless steel autoclave and heated for 7 h at 150 °C. Afterwards, the final product was separated by centrifugation method, washed thoroughly with ultrapure water and ethanol, and dried for 1 h at 60 °C. Finally, the white powder of ZnO nanoparticle was successfully obtained.

2.3. Graphene oxide (GO) preparation

The modified Hummer's method was performed to synthesize GO [27]. Briefly, 5g of graphite powder, 2.5 g of sodium nitrate (NaNO_3) and 12 mL of concentrated sulphuric acid (H_2SO_4) were mixed and stirred for 1 h in an ice bath. Then, the oxidation agent of KMnO_4 (1.5 g) was gently added with constant stirring. The ice bath was removed, and then it was stirred at 40 °C for 2 h. Later, 50 mL of ultrapure water was slowly poured into the above solution and vigorously stirred for 30 min at 98 °C. The addition of ultrapure water (300 mL) was followed by 30% of H_2O_2 (20 mL) into the mixture, and the reaction process was stopped. The bottom end material was centrifuged and washed several times with ultrapure water until the pH of the supernatant was neutral. Finally, the brown powder of GO was obtained after dried for 2 h at 60 °C.

2.4. Electrode modification

The GO suspension was made by dispersing GO/ultrapure water (1 mg/1 mL) by sonication method (45 min). In the same manner, L-glutathione and ZnO suspension were also prepared. To prepare glutathione-GO composite, we sonicated the GO powder with glutathione (1:1) for 2 h and stirred for 30 min at 60 °C, and then got a homogeneous stable suspension. The glutathione-GO/ZnO nanocomposite was prepared by sonicating 30 μ L of ZnO suspension and 70 μ L of glutathione-GO for 2 h. The bare GCE was polished with 1.0, 0.3 and 0.05 μ m alumina slurry sequentially. Then it was sonicated for 10 min with ethanol followed by ultrapure water. Subsequently, 10 μ L of glutathione-GO/ZnO nanocomposite was coated on a cleaned GCE surface and then dried at room temperature. This GCE was named as glutathione-GO/ZnO/GCE, and likewise GO/GCE, glutathione-GO/GCE, glutathione/GCE and ZnO/GCE were also fabricated.

2.5. Preparation of real samples

Dolonex DT tablet, water and blood serum samples were taken for direct detection of piroxicam. The blood serum sample was diluted with buffer solution in a 1:25 ratio and a known quantity of analyte was added for the determination study. A 1 g of finely ground Dolonex DT tablet was weighted and dissolved in 20 mL of PB solution/methanol (1:1). The solution was stirred and the remaining residue was removed by filtering. Then, the adequate volume of clear solution was diluted by buffer. The collected water sample was also filtered, diluted with PB solution and spiked with requisite range of analyte.

3. Result and discussion

3.1. FE-SEM

Fig. 1 depicts the FE-SEM photos of GO (A), glutathione-GO (B), ZnO (C) and glutathione-GO/ZnO nanocomposite (D). The GO surface texture shows thin crumpled graphene sheets, which are wrinkled and closely stacked with a multilayer structure (Fig. 1A). This probably resulted from lots of functional groups existing in the interlayer nanosheets. In comparison to GO, the fluffy exfoliated individual sheets are easily identifiable for glutathione-GO (Fig. 1B).

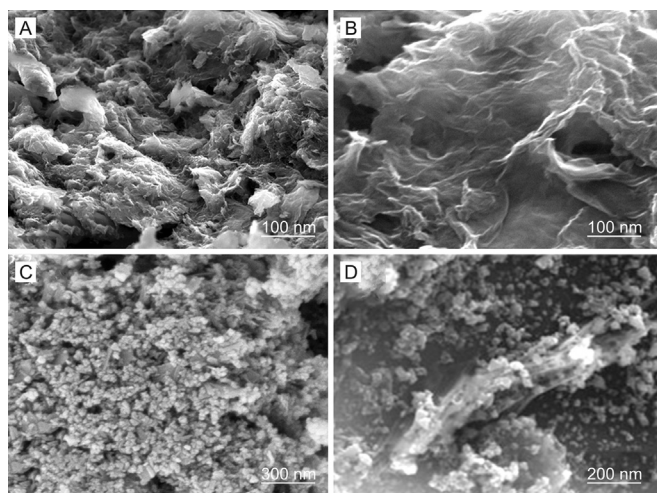


Fig. 1. FE-SEM photos of (A) GO, (B) glutathione-GO, (C) ZnO and (D) glutathione-GO/ZnO nanocomposite.

The formation of corrugated paper-like nanosheets demonstrated the reduction of GO through the interaction of GSSG via hydrogen bonding. The typical grain particle like morphology was observed for ZnO (Fig. 1C). Fig. 1D vividly shows that the ZnO nanoparticles uniformly grow on the wavy surface of glutathione-GO sheets. The participation of glutathione-GO in nanocomposite significantly prevented the agglomeration of nanoparticles. Therefore, the FE-SEM analysis confirms the formation of glutathione-GO/ZnO nanocomposite.

3.2. XRD analysis

XRD technique was performed to inspect the interlayer metamorphosis of the prepared samples. Fig. 2A depicts the XRD results of graphite, GO, glutathione-GO, ZnO and glutathione-GO/ZnO nanocomposite. In the XRD pattern of pristine graphite, an incisive peak (002) appeared at $2\theta = 26.6^\circ$ with d-spacing of 0.35 nm. In GO, the peak related to (002) pristine graphite completely vanished and a new peak (001) at $2\theta = 10.8^\circ$ appeared with an increased d-spacing of 0.79 nm. The introduction of functional groups on the nanosheets and intercalation of water molecules were responsible for the increment in d-spacing. After the addition of glutathione in GO, the sharp peak at $2\theta = 10.8^\circ$ of GO disappeared and a broad peak emerged at 25.2° with diminished d-spacing indicating the partial elimination of oxygen species and complete exfoliation of the layered GO structure [28,29]. Whereas, the ZnO spectrum reflects seven dominant peaks at (100), (002), (101), (102), (110), (103) and (112) plans which precisely match with typical hexagonal wurtzite type of bulk ZnO (No: 36–145). The absence of other peaks indicates the purity of the prepared ZnO sample. But the glutathione-GO/ZnO nanocomposite shows similar diffraction pattern of ZnO along with the appearance of new hump at 25.4° , evidencing the existence of ZnO and glutathione-GO. Further, the decreased intensities of all specific diffraction peaks related to ZnO and glutathione-GO in glutathione-GO/ZnO demonstrate the success of nanocomposite formation (Enlarged figure shown in Fig. S1).

3.3. FTIR characterization

Fig. 2B represents the FTIR spectra of GO, glutathione-GO, ZnO and glutathione-GO/ZnO nanocomposite. In GO spectrum, the fairly broad and intense peak appears at $\sim 3600\text{--}3436\text{ cm}^{-1}$ which is responsible for stretching vibration of hydroxyl group, indicating the presence of OH and/or COOH functional groups on the graphitic layer. Other low intense peaks at 1740, 1599 and 1035 cm^{-1} correspond to the stretching of carboxylic acid group, C–C stretching vibration of the graphitic domain and –CO stretching vibrations of alkoxy group, respectively [27]. For glutathione-GO, the low intense broad peak at 3545 cm^{-1} and the diminished peak at 1740 cm^{-1} evidence the decomposition of carboxylic groups, which may be due to the effective hydrogen bonding and electrostatic interaction of glutathione on the surface of GO. Besides, a sharp peak at 1550 cm^{-1} and a new peak at 1179 cm^{-1} indicate the restoration of sp^2 carbon honeycomb structure and the existence of O–H group at the alleviated edges of the graphitic layer, respectively. In ZnO spectrum, the zinc-oxygen (Zn–O) bond vibration appears at 598 cm^{-1} . It can be seen that the blended IR characteristic peak of glutathione-GO (C–C at 1555 cm^{-1} and –OH at 3590 cm^{-1}) and ZnO (Zn–O at 572 cm^{-1}) is clearly observed in glutathione-GO/ZnO spectrum. Thus, the FTIR results prove the successful preparation of glutathione-GO/ZnO nanocomposite, which well consist with FE-SEM and XRD results.

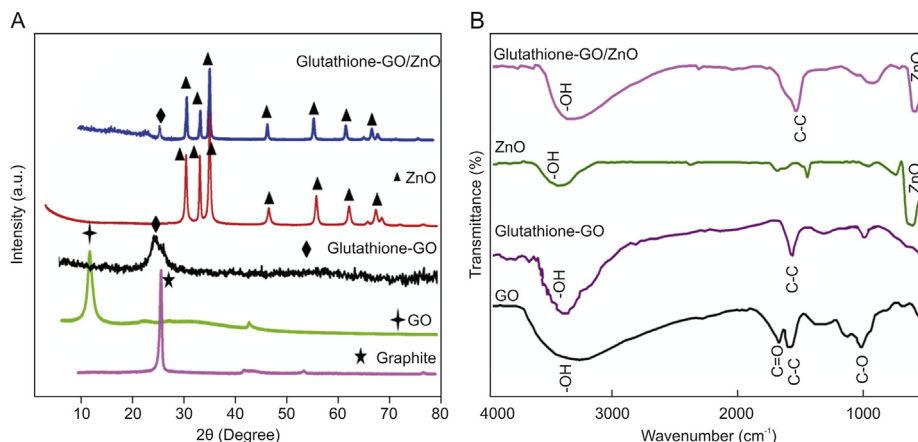


Fig. 2. (A) XRD patterns of graphite, GO, glutathione-GO, ZnO and glutathione-GO/ZnO nanocomposite. (B) FTIR spectrum of GO, glutathione-GO, ZnO and glutathione-GO/ZnO nanocomposite.

3.4. XPS analysis

One of the best surface analytical techniques of XPS was employed to understand chemical bonding state of elements and the nature of functional groups existing in the prepared nanocomposite. Fig. 3 illustrates C 1s data of GO (A), glutathione-GO (B) and survey spectra of GO and glutathione-GO/ZnO nanocomposite (C). The C 1s spectrum of GO displays four kinds of characteristic peaks corresponding to oxygen related functional groups such as epoxy, carbonyl and hydroxyl groups. The peak appeared at 284.5 eV is assigned to the sp^2 carbon of C–C bonding in the graphitic layer and the other three peaks at 286.6, 288.1 and 288.7 eV are attributed to the functional groups of C–O, C=O and O–C=O, respectively (Fig. 3A). According to Fig. 3B, the decreased C 1s peak intensity of glutathione-GO/ZnO when compared to GO

exposes the deoxygenating potential of glutathione [23]. The survey spectrum of glutathione-GO/ZnO exhibits low and high energy Zn related peaks, O 1s, and C 1s peaks with receded intensity acknowledging the functional group interactions in the nanocomposites (Fig. 3C).

3.5. CV and EIS behavior of glutathione-GO/ZnO nanocomposite

The electrochemical behaviour of bare and various modified electrodes was evaluated by CV and EIS in the presence of commonly used $[\text{Fe}(\text{CN})_6]^{3-/4-}$ solution. CV responses of bare GC, glutathione, GO, ZnO, glutathione-GO, and glutathione-GO/ZnO nanocomposite modified electrodes are shown in Fig. S2A. At bare GCE, a pair of redox peaks was observed which illustrates the penetrable nature of bare GCE towards 1 mM of $[\text{Fe}(\text{CN})_6]^{3-/4-}$. At

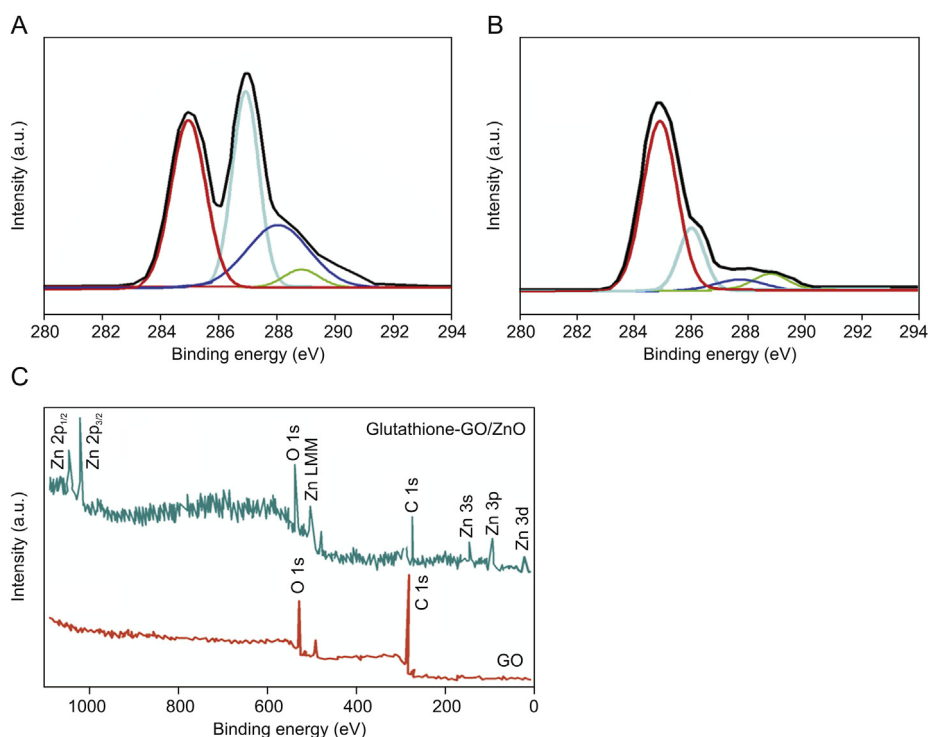


Fig. 3. The C 1s XPS spectra of (A) GO and (B) glutathione-GO. (C) Survey spectra of GO and glutathione-GO/ZnO nanocomposite.

GO/GCE, almost no redox peak was received, apparently due to electrostatic repulsion from intrinsic anionic functional groups of GO against anionic $[\text{Fe}(\text{CN})_6]^{3-/4-}$ ions. After addition of glutathione in GO, the peak current response was significantly enhanced, because most of the oxygen functional moieties of GO were effectively reduced by glutathione which can facilitate a good electron transfer pathway. The ZnO/GCE showed a defused peak, probably as a result of an aggregation of nanoparticles on the surface of GCE. On the other hand, a pair of well resolved redox peaks with remarkably enhanced current response was obtained at glutathione-GO/ZnO/GCE. Therefore, the nanocomposite modified electrode was highly conductive and allowed the electron transfer more easily than other GCEs. The electrode active surface area was calculated from the Randles-Sevcik [27] Eq. (1).

$$I_p = (2.59 \times 10^5) (A) (D^{1/2}) (n^{3/2}) (\nu^{1/2}) (C) \quad (1)$$

where, I_p refers to the anodic peak current, A is surface area of the electrode, D represents the diffusion coefficient of electrolyte ($D = 7.6 \times 10^{-6}$ cm²/s), n is the number of electrons transferred in a reaction, ν is the scan rate, and C represents the concentration of $[\text{Fe}(\text{CN})_6]^{3-/4-}$. The active surface area of glutathione-GO/ZnO/GCE was calculated as 0.0974 cm².

EIS approach was very useful in analyzing the interaction of electrode/modifier/electrolyte interface [30]. The charge transfer resistance (R_{CT}) value was measured from semicircle diameter in the Nyquist plots (Fig. S2B) using Randles equivalent circuit model [R_{CT} (Q)_{CPE} R_s (O)]. The R_{CT} data of various modified electrodes indicate the direct diffusion of $[\text{Fe}(\text{CN})_6]^{3-/4-}$ into the modified electrode through pinholes or collapsed sites. We acquired R_{CT} values of 5.8 k Ω , 4.3 k Ω , 3.8 k Ω , and 2.8 k Ω for GO, glutathione, ZnO, and glutathione-GO, respectively. A very small R_{CT} value of 1.4 k Ω was obtained for glutathione-GO/ZnO nanocomposite modified electrode, which indicates the electrocatalytic effect of ZnO and efficient electron transfer ability of glutathione-GO.

3.6. Electrochemical behavior of piroxicam

Fig. 4 depicts the CV response of 100 μM piroxicam on bare, glutathione-GO, ZnO and glutathione-GO/ZnO modified GCE, which were recorded over the potential range of 0.2–0.9 V with 50 mV/s of scan rate. It can be clearly observed that the current response had a significant improvement in both glutathione-GO and ZnO modified electrode when compared to bare GCE (Fig. 4).

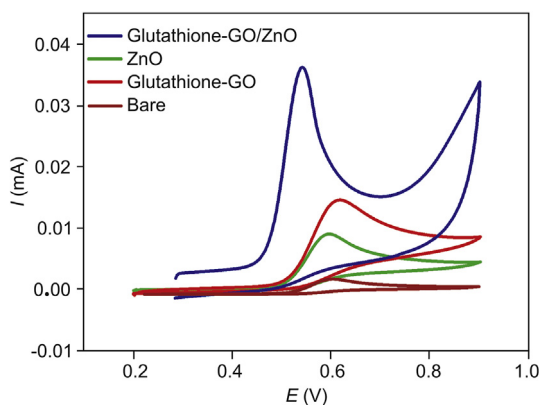


Fig. 4. CV behavior of 100 μM piroxicam on bare, glutathione-GO, ZnO and glutathione-GO/ZnO modified GCE recorded at the scan rate of 50 mV/s.

Nonetheless, the glutathione-GO/ZnO modified GCE exhibits phenomenal current response with incisive oxidation amplitude at 0.52 V which is 3 folds greater than glutathione-GO/GCE. This extraordinary output is possibly due to the stable electronic properties and nano-size effect of ZnO and more importantly, the glutathione in GO can increase the interlayer distance of graphitic sheets and concurrently participate in the partial reduction of GO. It could facilitate the high surface area containing porous structure, making it more responsive towards the electron transfer process between the electrode/electrolyte interfaces.

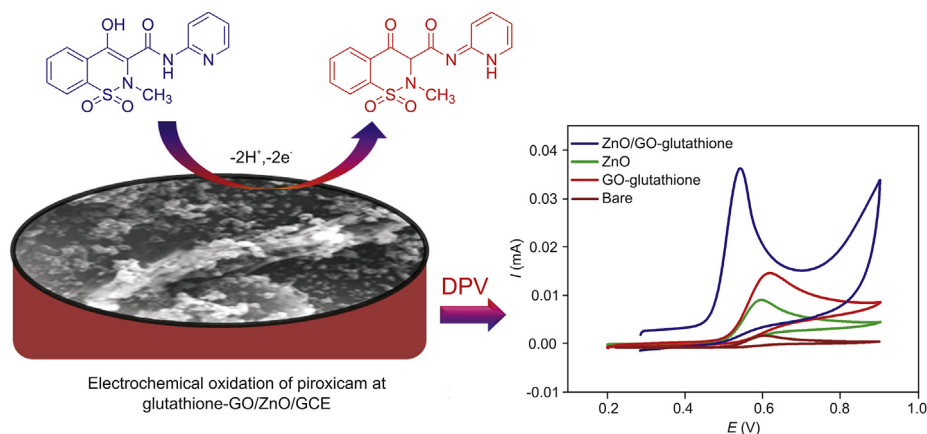
The impact of scan rate on the detection of 100 μM piroxicam was inspected at glutathione-GO/ZnO modified electrode by CV (scan rate ranging from 10 to 100 mV/s). As seen in Fig. S3A, a good linear relation was received for the plot of oxidation current response versus scan rates, evidencing that the electrochemical oxidation of piroxicam at glutathione-GO/ZnO/GCE was adsorption controlled system [31]. Additionally, the peak potential was gradually moved to more positive side, indicating the irreversible reaction of piroxicam (Fig. S3B). The electro-oxidation of piroxicam at glutathione-GO/ZnO/GCE is shown in Scheme 1.

The optimization of solution pH is a very important factor for the sensitive and selective determination of piroxicam. The effect of solution pH on the electrochemical response of piroxicam was investigated using DPV technique. When increasing the solution pH (4.0–9.0), the peak potential of piroxicam at glutathione-GO/ZnO/GCE was shifted to the more negative side (Fig. S4B), confirming that the electrochemical reaction is relative to proton exchange [32]. A linear relationship between peak potential and pH was observed with a correlation coefficient of 0.997. In Fig. S4A, the current response of piroxicam was increased with the increment of solution pH value from 4.0 to 7.0 and decreased thereafter. Consequently, pH value of 7.0 was fixed as an optimal pH for future investigations.

The influence of accumulation potential on piroxicam detection was examined from 0 to 0.9 V potential ranges. There was no specific change in current response or peak potential (figure not shown). Not like accumulation potential, the height of peak current was notably affected by accumulation time. It can be seen in Fig. S5 that the oxidation current rose initially with increased accumulation time, and after 90 s it maintained the same level. This shows the rapidity of piroxicam approaching close to the active sites and its saturation point. Thus, the optimum accumulation time of 90 s was selected for the entire experiments.

3.7. Voltammetric determination of piroxicam at glutathione-GO/ZnO modified electrode

In view of achieving higher sensitivity, DPV technique was adopted to perform the electrochemical determination of piroxicam at glutathione-GO/ZnO/GCE. Under the controlled experiment condition, a sequence of DPVs was recorded for various concentrations of piroxicam and the corresponding analytical curves are shown in Fig. 5A. It is clear that the peak intensities were linearly proportional to the concentrations of drug in the range of 1–500 μM . The standard plot (Fig. 5B) displays two linear relationships with piroxicam concentrations over the range of 0.1–100 μM and 100–500 μM , respectively. From the first linear segment, LOD and sensitivity of sensor were calculated as 1.8 nM ($S/N = 3$) and 0.2 $\mu\text{A}/\mu\text{M}\cdot\text{cm}^2$, respectively. Through these performances, the proposed novel electrode was comparable and even superior to that in earlier reported literature [32–40] and the comparison is shown in Table 1. This magnificent performance is attributed to the following synergetic electro-catalytic effects of constituents in the glutathione-GO/ZnO nanocomposite. One is the reduction of GO using L-glutathione providing many nanocavities



Scheme 1. Schematic diagram for the electro-oxidation of piroxicam at glutathione-GO/ZnO/GCE.

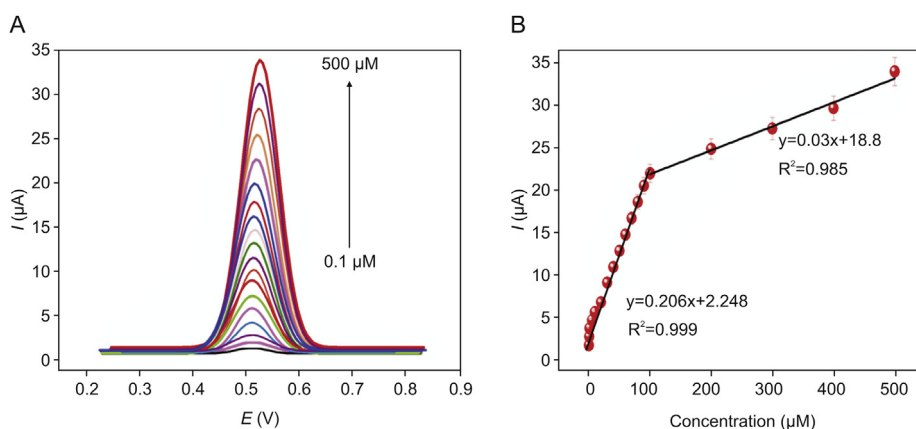


Fig. 5. (A) DPV determination of piroxicam at glutathione-GO/ZnO modified GCE in the concentration range of 0.1–500 μM . (B) The calibration plot between concentrations vs. anodic peak currents of piroxicam.

Table 1

Comparison for the determination of piroxicam with different modified electrodes.

Electrode	Method	Linear range (μM)	LOD (μM)	Refs.
CD/CPE	FFTCV	0.01–2.4	0.005	[32]
AgNPs-SWCNTs-rGO/GCE	LSV	1.5–400	0.5	[33]
PAA-FeNPs-MWCNTs/GCE	DPV	0.2–80	0.045	[34]
BNP-CP	ASDPV	0.5–100	0.0001	[35]
GCE/ZnO-Pd/CNTs	DPV	0.1–90	0.04	[36]
Pt-N-rGO-SWCNTs/GCE	DPV	0.06–60	0.015	[37]
GrO-CD/CPE	SWV	1–15	0.105	[38]
CILE	DPV	0.2–60	0.04	[39]
DF-AuNps	DPV	0.5–50	0.05	[40]
glutathione-GO/ZnO/GCE	DPV	0.1–500	0.0018	This work

CD: β -cyclodextrine; CPE: carbone paste electrode; FFTCV: fast fourier transform cyclic voltammetry; AgNPs: silver nanoparticles; SWCNTs: single walled carbon nanotubes; rGO: reduced graphene oxide; GCE: glassy carbon electrode; PAA: poly-aspartic acid; FeNP: Fe_3O_4 nanoparticle; MWCNTs: multiwalled carbon nanotubes; BNP: boehmite nanoparticles; CNTs: carbon nanotubes; Pt-N: Pt nanoparticles supported on nitrogen; GrO: graphite oxide; CILE: carbon ionic liquid electrode; DF-AuNps: diflunisal-derived gold nanoparticles.

and numerous catalytic active sites, which is too potent in expediting the electron transfer and adsorption of piroxicam. In reduced form, each glutathione molecule is able to release a proton which may possibly bond with another reactive glutathione to yield a glutathione disulfide (GSSG). It is well known that the reduced GO has residual $-\text{OH}$ polarity of carboxylic acid groups at edges of their sheets, and it can form a hydrogen bond with the negatively charged carboxylate group of GSSG. This interaction may disturb

the π - π stacking between every two graphene nanosheets, which can ultimately prevent the restacking process. Thus, the probable interlayer linked GSSG-graphene provided a larger active surface area and a favourable nano-environment with high electron shifting feature facilitated the rapid and accurate piroxicam detection. Besides, the unique features of ZnO nanoparticles like good adsorption and binding ability, high surface to volume ratio and suitable nano-size morphology could augment the loading amount

of piroxicam on the glutathione-GO/ZnO nanocomposite modified surface. Therefore, the proposed modifier could act as a simple and reliable avenue for the enhanced electrochemical determination of piroxicam. Scheme 2 represents the possible interaction of glutathione-GO/ZnO nanocomposite which is similar to that in previous reported literature [28].

3.8. Deletion of interferent effects on the electrochemical tracing of piroxicam

The concurrent determination of piroxicam along with AA and UA is one of the main goals of this work, because their peak potentials are very close to piroxicam potential which may possibly interfere the electrochemical responses of piroxicam. Fig. S6 shows the DPV determination of piroxicam in the presence of AA and UA. The concentration of piroxicam, AA, and UA was concurrently added and three well defined oxidation peaks were obtained at the potentials of 210, 400 and 520 mV for AA, UA and piroxicam, respectively. The peak current intensities were linearly proportional to the concentration of these analytes. The obtained potential differences between these analytes were huge enough for the simultaneous determination of these analytes in a mixture. The sensitivity was calculated as $0.201 \mu\text{A}/\mu\text{M}\cdot\text{cm}^2$ for piroxicam in the presence of AA and UA. This value is virtually the same as the sensitivity of individual piroxicam determination ($0.206 \mu\text{A}/\mu\text{M}\cdot\text{cm}^2$). Therefore, these results evidence that the proposed novel modified electrode is more independent for the electrochemical determination of piroxicam, AA, and UA, and the simultaneous determination of their mixtures is feasible without any interferences.

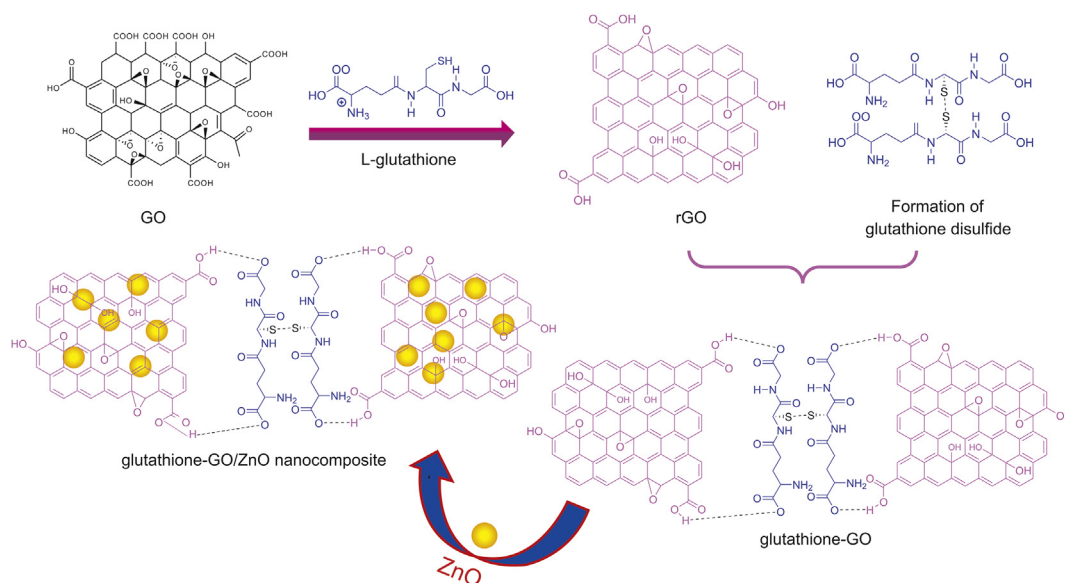
3.9. Stability, reproducibly and anti-interference ability of glutathione-GO/ZnO/GCE

In order to ascertain the reproducibility of glutathione-GO/ZnO/GCE towards piroxicam sensing, a series of eight individually modified electrodes were prepared and tested under the same optimum conditions in the presence of $100 \mu\text{M}$ piroxicam (Fig. S7).

The observed relative standard deviation (RSD) of 2.36% indicates the precision of the sensing system. Furthermore, the storage stability of the sensor was examined. The electrochemical detection of $100 \mu\text{M}$ piroxicam at glutathione-GO/ZnO/GCE was initially measured. After that the electrode was immersed in buffer and stored for 21 days at normal laboratory condition. It could retain 97% of its initial response without any changes in peak potential for the determination of piroxicam (Fig. S8). The interference survey was also performed to explore the selectivity of the present electrode. The commonly found species in pharmaceutical products such as magnesium stearate, lactose monohydrate, talc and starch (50-fold concentration) were studied in the presence of $100 \mu\text{M}$ piroxicam. Likewise, 40-fold excess concentrations of other biological interfering compounds such as glucose, urea, dopamine, folic acid, glycine and L-lysine were also studied. The availability of other interfering compounds did not perturb the height and position of peak current and potential of piroxicam, respectively (figure not shown). Thus, these obtained results strongly show the agreeable long-term stability, reproducibility, and selectivity of the glutathione-GO/ZnO/GCE.

3.10. Real sample application

The direct analysis of piroxicam in Dolonex DT tablet (bought from local drug store), human blood (collected from local government hospital) and water (collected from local place) were verified by the proposed modified electrode. The standard addition method was adopted to analyze these practical samples and the obtained findings were cross checked by HPLC results (Table 2). As shown in Table 2, the average recovery percentages of 99.2%, 100.6% and 99.3% were observed for tablet, blood serum and water samples, respectively. It seems that the presence of various components in the blood serum, water and tablet has no significant effects on the electrochemical detection of piroxicam. Therefore, the acquired recoveries demonstrate that the glutathione-GO/ZnO modified electrode is a reliable approach to the analysis of real samples in different matrices.



Scheme 2. Schematic diagram for the possible interaction of glutathione-GO/ZnO nanocomposite.

Table 2
Determination of piroxicam in blood serum, Dolonex DT tablet and water sample at glutathione-GO/ZnO modified GCE.

Real samples	Added (μM)	Found (μM)		Recovery (%)
		Comparative method (HPLC)	Proposed sensor (DPV)	
Blood serum	0	—	—	—
	1	1.01	0.98	102
	5	4.99	5.04	99.2
Dolonex DT tablet	0	5.01	4.98	—
	1	6.05	6.02	99.6
	5	9.99	10.12	98.8
Water	0	—	—	—
	1	0.99	1.02	98
	5	5.01	4.97	100.6

4. Conclusion

In the present study, a facile and low-cost production of reduced GO was prepared by using environment friendly L-glutathione. The result of FE-SEM clearly evidenced the formation of corrugated paper-like individual sheets of glutathione-GO. This confirmed that L-glutathione and its oxidative product could act as a reducing agent concurrently stabilizing the single layer formation. The prepared glutathione-GO was successfully utilized for the preparation of novel glutathione-GO/ZnO nanocomposite. The characterization of XRD, FTIR, FE-SEM and XPS results indicated the success of nanocomposite preparation. The glutathione-GO/ZnO modifier performed as an accurate sensing platform for the high-performance piroxicam sensor. Its numerous catalytic active sites, larger active surface area and favourable nano-size morphology can access a greater number of piroxicam molecules on the electrode surface. In addition, the proposed sensing system exhibited excellent selectivity, reproducibility, and long-term stability, and it can effectively ignore the interfering compounds commonly present in the pharmaceutical tablets and biological fluids. The sensor further manifested potent capability to detect piroxicam in real samples like human blood serum, pharmaceutical tablet and water with reliable accuracy. Thus, the practical viability and affordable cost of electrode modifier may popularize this sensor for the high-performance piroxicam sensor.

Declaration of competing interest

The authors declare that there are no conflicts of interest.

Acknowledgments

This work was supported by SERB (Science and Engineering Research Board), New Delhi, India [File. No: EMR/2014/000020].

Appendix A. Supplementary data

Supplementary data to this article can be found online at <https://doi.org/10.1016/j.jpha.2020.02.001>.

References

- J.G. Hardman, L.E. Limbird, A. Goodman-Gilman, *The Pharmacological Basis of Therapeutics*, McGraw Hill, New York, 2001, pp. 1295–1312.
- Y.H. Chang, S.H. Dromgoole, in: H.E. Paulus, D.E. Furst, S.H. Dromgoole (Eds.), *Drugs for Rheumatic Disease*, Churchill Livingstone, New York, 1987, pp. 389.
- A. Babaei, M. Sohrabi, M. Afrasiabi, A sensitive simultaneous determination of epinephrine and piroxicam using a glassy carbon electrode modified with a nickel hydroxide nanoparticles/multiwalled carbon nanotubes composite, *Electroanalysis* 24 (2012) 2387–2394.
- F. Bessone, Non-steroidal anti-inflammatory drugs: what is the actual risk of liver damage, *World J. Gastroenterol.* 16 (2010) 5651–5661.
- Database of Prevalence of arthritis rising among Indians. <https://www.deccanchronicle.com/lifestyle/health-and-wellbeing/121017/prevalence-of-arthritis-rising-among-indians.html>.
- J.L. Manzoori, M. Amjadi, Spectrofluorimetric determination of piroxicam in pharmaceutical preparations and spiked human serum using micellar media, *Microchim. Acta.* 143 (2003) 39–44.
- S.M. Al-Kindy, A. Al-Wishahi, F.E.O. Suliman, A sequential injection method for the determination of piroxicam in pharmaceutical formulations using europium sensitized fluorescence, *Talanta* 64 (2004) 1343–1350.
- B.S. Nagaralli, J. Seetharamappa, M.B. Melwanki, Sensitive spectrophotometric methods for the determination of amoxicillin, ciprofloxacin and piroxicam in pure and pharmaceutical formulations, *J. Pharmaceut. Biomed. Anal.* 29 (2002) 859–864.
- A.J. Nepote, L. Vera-Candiotti, M.R. Williner, et al., Development and validation of chemometrics-assisted spectrophotometry and micellar electrokinetic chromatography for the determination of four-component pharmaceuticals, *Anal. Chim. Acta* 489 (2003) 77–84.
- M. Sultan, G. Stecher, W.M. Stoggl, et al., Sample pretreatment and determination of non steroidal anti-inflammatory drugs (NSAIDs) in pharmaceutical formulations and biological samples (blood, plasma, erythrocytes) by HPLC-UV-MS and μ -HPLC, *Curr. Med. Chem.* 12 (2005) 573–588.
- M. Starek, J. Krzek, M. Tarsa, et al., Determination of piroxicam and degradation products in drugs by TLC, *Chromatographia* 69 (2009) 351–356.
- A. Doliwa, S. Santoyo, M.A. Campanero, et al., Sensitive LC determination of piroxicam after in vitro transdermal permeation studies, *J. Pharmaceut. Biomed. Anal.* 26 (2001) 531–537.
- Y.L. Chen, S.M. Wu, Capillary zone electrophoresis for simultaneous determination of seven nonsteroidal anti-inflammatory drugs in pharmaceuticals, *Anal. Bioanal. Chem.* 381 (2005) 907–912.
- H. Karimi-Maleh, F. Tahernejad-Javazmi, N. Atar, et al., A novel DNA biosensor based on a pencil graphite electrode modified with polypyrrole/functionalized multiwalled carbon nanotubes for determination of 6-mercaptopurine anticancer drug, *Ind. Eng. Chem. Res.* 54 (2015) 3634–3639.
- M. Ramrakhiani, Nanostructures and their applications, *Recent Res. Sci. Technol.* 4 (2012) 14–19.
- K. Ghanbari, S. Bonyadi, An electrochemical sensor based on reduced graphene oxide decorated with polypyrrole nanofibers and zinc oxide–copper oxide p–n junction heterostructures for the simultaneous voltammetric determination of ascorbic acid, dopamine, paracetamol, and tryptophan, *New J. Chem.* 42 (2018) 8512–8523.
- M.M. Rahman, H.M. Marwani, F.K. Algethami, et al., Xanthine sensor development based on ZnO–CNT, ZnO–CB, ZnO–GO and ZnO nanoparticles: an electrochemical approach, *New J. Chem.* 41 (2017) 6262–6271.
- S. Priyadarsini, S. Mohanty, S. Mukherjee, et al., Graphene and graphene oxide as nanomaterials for medicine and biology application, *J. Nanostructure. Chem.* 8 (2018) 123–137.
- C.I. Justino, A.R. Gomes, A.C. Freitas, et al., Graphene based sensors and biosensors, *TrAC Trends Anal. Chem.* 91 (2017) 53–66.
- M.L. Yola, V.K. Gupta, T. Eren, et al., A novel electro analytical nanosensor based on graphene oxide/silver nanoparticles for simultaneous determination of quercetin and morin, *Electrochim. Acta* 120 (2014) 204–211.
- N.F. Atta, A. Galal, E.H. El-Ads, Graphene—a Platform for Sensor and Biosensor Applications, in: *Biosensors-Micro and Nanoscale Applications*, InTech, 2015, pp. 37–84.
- V. Georgakilas, J.N. Tiwari, K.C. Kemp, et al., Non covalent functionalization of graphene and graphene oxide for energy materials, biosensing, catalytic, and biomedical applications, *Chem. Rev.* 116 (2016) 5464–5519.
- T.A. Pham, J.S. Kim, J.S. Kim, One-step reduction of graphene oxide with L-glutathione, *Colloids Surf. A* 384 (2011) 543–548.
- G.A. Bagiyani, I.K. Koroleva, N.V. Soroka, et al., Oxidation of thiol compounds by molecular oxygen in aqueous solutions, *Russ. Chem. Bull.* 52 (2003)

- 1135–1141.
- [25] M.J. Fernández-Merino, L. Guardia, J.I. Paredes, et al., Vitamin C is an ideal substitute for hydrazine in the reduction of graphene oxide suspensions, *J. Phys. Chem. C* 114 (2010) 6426–6432.
- [26] C. Zhu, S. Guo, Y. Fang, et al., Reducing sugar: new functional molecules for the green synthesis of graphene nanosheets, *ACS Nano* 4 (2010) 2429–2437.
- [27] N. Dhanalakshmi, T. Priya, N. Thinakaran, Highly electroactive Ce-ZnO/rGO nanocomposite: ultra-sensitive electrochemical sensing platform for carbamazepine determination, *J. Electroanal. Chem.* 826 (2018) 150–156.
- [28] S. Chhetri, N.C. Adak, P. Samanta, et al., Investigation of the mechanical and thermal properties of l-glutathione modified graphene/epoxy composites, *Compos. B Eng.* 143 (2018) 105–112.
- [29] R. Hrdy, H. Kynclova, J. Drbohlavova, et al., Electrochemical impedance spectroscopy behaviour of guanine on nanostructured planar electrode, *Int. J. Electrochem. Sci.* 8 (2013) 4384–4396.
- [30] Z. Zhao, J. Zhang, W. Wang, et al., Synthesis and electrochemical properties of Co₃O₄-rGO/CNTs composites towards highly sensitive nitrite detection, *Appl. Surf. Sci.* 485 (2019) 274–282.
- [31] A. Wong, A.M. Santos, O. Fatibello-Filho, Determination of piroxicam and nimesulide using an electrochemical sensor based on reduced graphene oxide and PEDOT: PSS, *J. Electroanal. Chem.* 799 (2017) 547–555.
- [32] P. Norouzi, N. Ghaheeri, β -Cyclodextrine modified carbon paste electrode as a selective sensor for determination of piroxicam using flow injection cyclic voltammetry, *Anal. Bioanal. Electrochem.* 3 (2011) 87–101.
- [33] J.W. Zhang, R.F. Li, L. Yao, et al., Highly sensitive determination of piroxicam using a glassy carbon electrode modified with silver nanoparticles dotted single walled carbon nanotubes-reduced graphene oxide nanocomposite, *J. Electroanal. Chem.* 823 (2018) 1–8.
- [34] A. Babaei, M. Afrasiabi, H. Moghanian, A new sensor based on the glassy carbon electrode modified with poly aspartic acid-Fe₃O₄ nanoparticle/multi-walled carbon nanotubes composite for a selective simultaneous determination of piroxicam and clopidogrel in the presence of uric acid, *Anal. Bioanal. Electrochem.* 9 (2017) 741–761.
- [35] M.B. Gholivand, G. Malekzadeh, A.A. Derakhshan, Boehmite nanoparticle modified carbon paste electrode for determination of piroxicam, *Sens. Actuators. B Chem.* 201 (2014) 378–386.
- [36] H. Karimi-Maleh, I. Sheikhshoaei, A. Samadzadeh, Simultaneous electrochemical determination of levodopa and piroxicam using a glassy carbon electrode modified with a ZnO–Pd/CNT nanocomposite, *RSC Adv.* 8 (2018) 26707–26712.
- [37] F.Y. Kong, R.F. Li, L. Yao, et al., Pt nanoparticles supported on nitrogen doped reduced graphene oxide-single wall carbon nanotubes as a novel platform for highly sensitive electrochemical sensing of piroxicam, *J. Electroanal. Chem.* 832 (2019) 385–391.
- [38] A.M. Santos, A. Wong, F.C. Vicentini, et al., Simultaneous voltammetric sensing of levodopa, piroxicam, ofloxacin and methocarbamol using a carbon paste electrode modified with graphite oxide and β -cyclodextrin, *Microchim. Acta.* 186 (2019), 174.
- [39] G. Ghobadpour, F. Farjami, F. Fasihi, Sensitive electrochemical monitoring of piroxicam in pharmaceuticals using carbon ionic liquid electrode, *Curr. Pharmaceut. Anal.* 15 (2019) 45–50.
- [40] T. Shaikh, F.N. Talpur, A.R. Khaskeli, et al., Ultrasensitive determination of piroxicam at diflunisal-derived gold nanoparticle-modified glassy carbon electrode, *J. Electron. Mater.* 46 (2017) 5957–5966.